Shape Optimization of Homogeneous Electromagnets *

Dalibor Lukáš
SFB F013, University of Linz, Austria
Dep. of Applied Mathematics, VŠB-TU Ostrava, Czech Rep.
e-mail: dalibor.lukas@vsb.cz

Abstract

Magneto-optical effects are investigated among others for their application in storage media. Measurements of Kerr effect requires magnetic field as homogeneous as possible. This is generated by so-called homogeneous electromagnets. The optimization aims at the optimal shape of the pole heads. The governing linear magnetostatic problem is approximated by the Finite Element Method (FEM) where quadratic triangular elements or edge elements are used in the 2-dimensional (2D) or 3-dimensional (3D) case, respectively. The solver is either a direct or multigrid Preconditioned Conjugate Gradient method (PCG) depending on the problem size. The Sequentional Quadratic Programming (SQP) method with the BFGS update of Hessian matrix was used for the optimization. We computed an optimized 2D coarse design which was produced afterwards. The measurements show significant improvements of the homogeneity. We also computed an optimized 2D fine design by a hierarchical strategy which is an iterative process where a coarse optimized shape is used as an initial design for the optimization on a finer grid. This approach seems to suit our class of problems very well. Finally, a coarse approximation of the 3D optimal shape was calculated.

1 Introduction

A number of applications needs homogeneous magnetic fields. They can be produced by electromagnets which impress such fields among the pole heads. These are called homogeneous electromagnets. In Fig. 1 there are two examples of them. In our case the homogeneous electromagnets are used for measurements of Kerr effect. The research of magneto-optical effects is interesting among others for the applications in magneto-optical storage media. This is investigated

*This research has been supported by the Austrian Science Fund FWF within the SFB "Numerical and Symbolic Computing" under the grant SFB F013

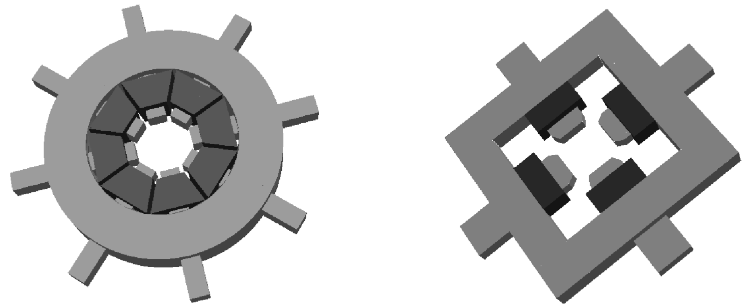

Figure 1: Homogeneous electromagnets - geometries “O-ring” (left) and “Maltese Cross” (right)

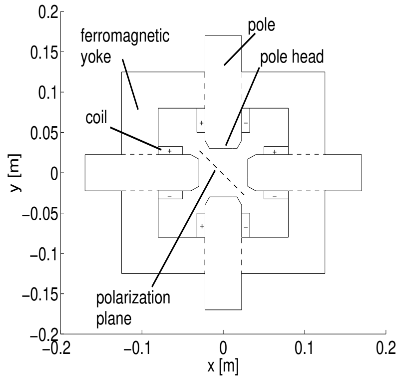

Figure 2: Cross section of the Maltese Cross

by the research team at Department of Physics at VŠB - Technical University of Ostrava, see [7], with whom we closely cooperate.

This paper presents mathematical modeling and shape optimization of electromagnets producing a homogeneous magnetic field among the pole heads. In particular, the results here are given for an electromagnet of a so-called Maltese Cross geometry. Considering this geometry, see Fig. 2, we will describe the physical problem. A sample of magneto-optical media is placed to the center. Rays coming to the center are polarized in the polarization plane by the magnetic field and then they reflect on the sample. The components of the reflected rays are measured. The field is to be as homogeneous as possible. By switching the sense of two currents we can polarize the rays in the orthogonal polarization plane as well. The device, see Fig. 2, consists of a ferromagnetic yoke, 4 poles, and 4 windings. The shape of the pole heads influences the magnetic field in the polarization plane significantly.

The general topics and the mathematical theory on shape optimization are covered in [2] and [10]. But, there are still only a few papers concerning with solving shape optimization problems governed by Maxwell equations. Particularly in magnetostatics there are theoretical works within the special research project SFB F003 "Optimization and Control" in Graz, Austria that are dealing with optimization of an electromagnet, see [5], [6]. On the other hand, a numerical solution of a practical problem, namely the TEAM (Testing Electromagnetic Analysis Methods) problem No. 25, see [11], is given in [1].

2 Setting of the Problem

2.1 Linear Magnetostatic Problem

First we introduce Maxwell equations for 3D linear magnetostatics. Let $\overline{\Omega} := \cup_{i=1}^{k} \overline{\Omega_i} \subset \mathbf{R}^3$ is a material-wise decomposition where Ω is bounded and Ω_i are Lipschitz domains such that

$$\mu(x, y, z) = \mu_i = \text{const.} \quad \text{for } i = 1, \ldots, k \tag{1}$$

denote domain-wise constant permeabilities of the appropriate materials. Further let $\mathbf{B}$ denotes the magnetic induction, $\mathbf{H}$ is the magnetic strength density, and $\mathbf{J}$ is the current density. Then the Maxwell equations take the form

$$\left.\begin{array}{rcl} \mathbf{rot}(\mathbf{H}) & = & \mathbf{J} \\ \mathbf{B} & = & \mu\mathbf{H} \\ \operatorname{div}(\mathbf{B}) & = & 0 \end{array}\right\} \text{ in } \Omega \ . \tag{2}$$

The corresponding boundary conditions are

$$\begin{array}{rcll} \mathbf{B} \cdot \mathbf{n} & = & 0 & \text{on } \Gamma_0 \ , \\ \mathbf{H} \times \mathbf{n} & = & \mathbf{0} & \text{on } \Gamma_1 \end{array} \tag{3}$$

such that $\partial\Omega = \overline{\Gamma_0} \cup \overline{\Gamma_1}$, $\Gamma_0 \cap \Gamma_1 = \emptyset$ and $\mathbf{n}$ is the unit normal vector of $\partial\Omega$. Finally the interface conditions

$$\begin{array}{rcl} [\mathbf{B} \cdot \mathbf{n}]_{i,j} & = & 0 \ , \\ [\mathbf{H} \times \mathbf{n}]_{i,j} & = & \mathbf{0} \end{array} \tag{4}$$

hold where $[\,]_{i,j}$ denotes the jump on the interface $\Gamma_{i,j} := \overline{\Omega_i} \cap \overline{\Omega_j}$ and $\mathbf{n}$ is the corresponding unit normal vector of $\Gamma_{i,j}$.

Now we introduce the magnetic vector potential $\mathbf{A}$ as follows:

$$\mathbf{rot}(\mathbf{A}) = \mathbf{B} \ , \ \operatorname{div}(\mathbf{A}) = 0 \ . \tag{5}$$

We obtain the reduced 2-dimensional problem by looking at a typical cross section $\Omega_{2\mathrm{D}}$. There hold $\mathbf{J} = (0, 0, \mathrm{J}(x, y))$, $\mathbf{B} = (\mathrm{B}_x(x, y), \mathrm{B}_y(x, y), 0)$, and the magnetic potential is uniquely given by

$$\mathbf{A} = (0, 0, u(x, y)) \ , \ \mathbf{B} = \left(\frac{\partial u}{\partial y}, -\frac{\partial u}{\partial x}, 0\right) \tag{6}$$

where u stands for the scalar potential.

Let $\Gamma_{0,2\mathrm{D}} := \Gamma_0 \cap \Omega_{2\mathrm{D}}$ and $\Gamma_{1,2\mathrm{D}} := \Gamma_1 \cap \Omega_{2\mathrm{D}}$ denote components of the boundary $\partial\Omega_{2\mathrm{D}}$. Applying (6) we arrive at the following 2D formulation of the linear magnetostatic problem :

$$\begin{aligned} -\mathrm{div}\left(\tfrac{1}{\mu}\nabla u\right) &= J \quad \text{in } \Omega_{2\mathrm{D}} \ , \\ u &= 0 \quad \text{on } \Gamma_{0,2\mathrm{D}} \ , \\ \tfrac{\partial u}{\partial n} &= 0 \quad \text{on } \Gamma_{1,2\mathrm{D}} \end{aligned} \tag{7}$$

with the interface conditions

$$\begin{aligned} [\nabla u \times \mathbf{n}]_{i,j} &= 0 \ , \\ \left[\left(\tfrac{1}{\mu}\nabla u \cdot \mathbf{n}\right)\right]_{i,j} &= 0 \ . \end{aligned} \tag{8}$$

Finally, we set the weak formulation. Since the domains are Lipschitz, we can form the Hilbert ansatz space

$$V := \{v \in H^1(\Omega_{2\mathrm{D}}) \mid v = 0 \text{ on } \Gamma_{0,2\mathrm{D}}\} \ . \tag{9}$$

Further let $J \in L^2(\Omega_{2\mathrm{D}})$. Since $1/\mu \in L^\infty(\Omega_{2\mathrm{D}})$ holds, the weak formulation of the 2D linear magnetostatic problem is well-defined and reads as follows :

$$\text{Find } u \in V \ : \ A(u,v) = b(v) \text{ for all } v \in V \tag{10}$$

where

$$A(u,v) := \int\limits_{\Omega_{2\mathrm{D}}} \frac{1}{\mu}.\nabla u.\nabla v \, dx \ , \ b(v) := \int\limits_{\Omega_{2\mathrm{D}}} \mathrm{J}.v \, dx \ . \tag{11}$$

2.2 Shape Optimization Problem

Let Γ_p is an area, e.g. the polarization plane in Fig. 2, in which dishomogeneities of the magnetic field are to be minimized. Let $\alpha_\mathrm{pole} \subset \partial\Omega_\mathrm{pole}$ is a shape of a pole head such that Ω_pole is the related pole domain. As the homogeneous magnetic field is possible to generate in different directions, the geometry of the considered electromagnets is always symmetric. That implies the same and symmetric shapes of the pole heads, i.e. $\alpha \equiv \alpha_\mathrm{pole}$. Independently of the geometry of an electromagnet, we consider the following optimization problem :

$$\min_{\alpha \in \mathcal{F}} \varphi(\alpha) \tag{12}$$

under the constraints

$$\mathrm{B}^\mathrm{avg}_\mathrm{min} \le \|\mathbf{B}^\mathrm{avg}_\alpha\| \ , \tag{13}$$

$$\alpha_\mathrm{l} \le \alpha \le \alpha_\mathrm{u} \tag{14}$$

where

$$\varphi(\alpha) := \frac{1}{\mathrm{meas}(\Gamma_\mathrm{p}).\,\|\mathbf{B}^\mathrm{avg}_\alpha\|^2} \cdot \int\limits_{\Gamma_\mathrm{p}} \|\mathbf{B}_\alpha(\mathbf{r}) - \mathbf{B}^\mathrm{avg}_\alpha\|^2 \, ds \ , \tag{15}$$

$$\mathbf{B}_\alpha^{\text{avg}} := \frac{1}{\text{meas}(\Gamma_{\text{p}})} \cdot \int_{\Gamma_{\text{p}}} \mathbf{B}_\alpha(\mathbf{r})\, ds \ , \tag{16}$$

$$\mathcal{F} := \{\alpha \subset \partial\Omega_{\text{pole}} \,|\, \alpha \text{ is Lipschitz continuous and symmetric}\} \ . \tag{17}$$

Note that (15) quantifies dishomogeneities along Γ_{p} and (13) prescribes a minimal magnetic field necessary for the polarization effect. Note also that this formulation is independent of the dimension.

3 Components of the Solver

The weak formulation of the 2-dimensional state problem is discretized by the Finite Element Method. We use quadratic triangular elements rather than linear ones to reach a better accuracy of the B-field. The arising linear system is basically solved by a Preconditioned Conjugate Gradient method. In the case when the number of unknowns is not too large, a direct solver is applied.

The optimization method is based on the Sequentional Quadratic Programming method with the BFGS update of Hessian matrix. The optimization problem described in Sect. 2.2 is discretized and design variables are coordinates of the nodes along the 1-dimensional shape design boundary α which is interpolated linearly. The integrals in (15) and (16) are replaced by a quadrature formula of the 0th order. Derivatives of the design are calculated by finite differences of the 3rd extrapolation order.

In shape optimization, once the shape has changed, the mesh is deformed. We use a simple strategy where nodes are displaced in a box around the pole head and in one direction only. The direction in which the nodes are displaced corresponds to the pole axis. Displacements of the inner nodes depend linearly on displacements of the shape boundary nodes. For large displacements overlapping elements can appear. This happens within the line-search procedure and we simply exclude such designs α for which an element has flipped. Since only symmetric shapes, see (17), are considered, the number of design variables is half the number of nodes along α. The shape α should also be Lipschitz continuous and, moreover, smooth enough because, otherwise, the linear magnetostatics is not valid and the shape is hardly producable. That is why, an additional constraint on the maximal curvature of α has been implemented. We interpolate the shape by piecewise cubic splines $\{\alpha_i\}$ and the curvature is calculated at each node along α. The constraint reads

$$-\frac{1}{\rho_{\min}} \le \frac{\alpha_i''(t_i)}{\sqrt{\left[1 + (\alpha_i'(t_i))^2\right]^3}} \le \frac{1}{\rho_{\min}} \quad \text{for all the design nodes } i \tag{18}$$

where $\rho_{\min} > 0$ is a minimal curvature radius, t is a parameter of the interpolating component $\alpha_i(t)$ of the shape, and $\alpha_i'(t)$ denotes the first derivative.

In order to get fine enough results efficiently, a hierarchical optimization strategy has been implemented. We say that the classical approach is applied if only one discretized optimization problem is solved, i.e. the topology of the mesh doesn't change. By the hierarchical strategy we mean that several discretized optimization problems are solved sequentially such that they approximate the problem finer at higher levels and the optimized design is used as the initial one at the next level. There are a refinement and a prolongation strategy involved. The refinement strategy deals with the refinement of the grid in order to get a better approximation of the cost functional and the constraints. In our case we refine the discretization of Γ_{p} and use a mesh generator for generating a finer mesh. The prolongation strategy prolonges the discretized optimization problem, particularly the optimized design, from a current grid to a finer one. It is done by using of an interpolation of the shape by cubic splines such that the middle points of the splines are used at the finer level. A stopping criterion of the hierarchical strategy can be a convergence criterion of the discretized cost function or a maximal number of levels. The hierarchical strategy is successful as far as the coarse optimized design approximates the fine one well.

4 An Application

In this section we present some results for an optimization of an electromagnet of a so-called Maltese Cross geometry. We are giving comparisons of a computed 2D optimized design to measurements. We are comparing classical and hierarchical approaches. Finally, a coarse optimized pole head is computed in 3D.

4.1 Setting of the Maltese Cross Problem

An electromagnet of the Maltese Cross geometry can be seen in Figs. 1, 2. First we set the state problem in 2D. As the shapes of the pole heads are the same and symmetric, the computational domain can be a quarter of the square in Fig. 2. According to Fig. 3 and Sec. 2, the material decomposition is $\overline{\Omega_{\mathrm{2D}}} := \overline{\Omega_0^1} \cup \overline{\Omega_0^2} \cup \overline{\Omega_{\mathrm{r}}} \cup \overline{\Omega_{\mathrm{J}+}} \cup \overline{\Omega_{\mathrm{J}-}}$. The Dirichlet and Neumann boundaries are $\Gamma_{0,\mathrm{2D}} := \Gamma_0 \cup \Gamma_{\mathrm{p}}$ and $\Gamma_{1,\mathrm{2D}} := \Gamma_1$, respectively. The ferromagnetic material is a kind of steel with the following permeability

$$\mu = \begin{cases} \mu_0 & \text{in } \overline{\Omega_{\mathrm{2D}}} \setminus \overline{\Omega_{\mathrm{r}}} \\ \mu_0.\mu_{\mathrm{r}} & \text{in } \overline{\Omega_{\mathrm{r}}} \end{cases} \quad , \; \mu_0 = 4\pi.10^{-7}\ \mathrm{H.m^{-1}} \quad , \; \mu_{\mathrm{r}} = 5100 \; .$$

The current density

$$\mathrm{J} = \begin{cases} 12.5\ \mathrm{MA.m^{-2}} & \text{in } \overline{\Omega_{\mathrm{J}_+}} \\ 0\ \mathrm{MA.m^{-2}} & \text{in } \overline{\Omega_{\mathrm{2D}}} \setminus \left(\overline{\Omega_{\mathrm{J}_+}} \cup \overline{\Omega_{\mathrm{J}_-}}\right) \\ -12.5\ \mathrm{MA.m^{-2}} & \text{in } \overline{\Omega_{\mathrm{J}_-}} \end{cases}$$

is given by the current $\mathrm{I} = 6.3$ A and by the wire diameter $\mathrm{d} = 0.8$ mm.

Then the weak formulation of the 2D state problem is given by (9)–(11). The shape optimization problem is described by (12)–(17) where α and Γ_{p} are introduced in Fig. 3, $\Omega_{\mathrm{pole}} := \Omega_{\mathrm{r}}$, $\alpha_{\mathrm{l}} = -0.05$ m, $\alpha_{\mathrm{u}} = -0.03$ m, and a typical average induction $\mathrm{B}_{\mathrm{min}}^{\mathrm{avg}} = 0.2$ T.

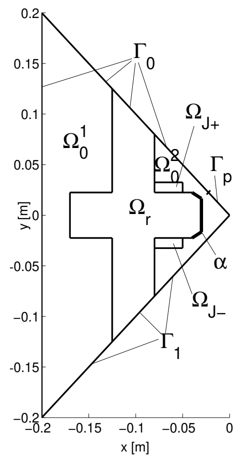

Figure 3: 2D computational domain of the Maltese Cross

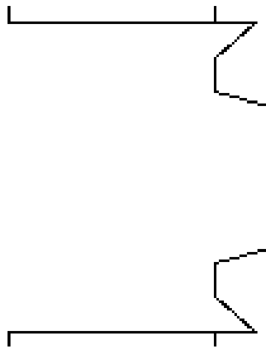

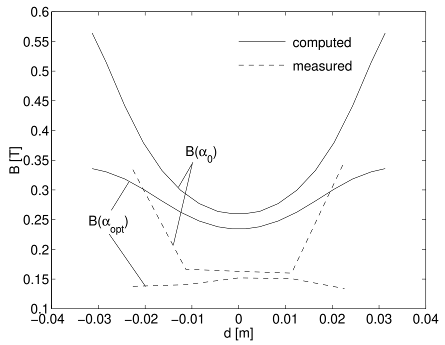

Figure 4: 2D coarse optimized design (left) and comparisons to measurements (right)

4.2 Comparisons of a 2D Coarse Optimized Design to Measurements

First, we present a 2D optimized design which we computed by the classical approach on a uniform mesh of the step size 2.5 mm and 25600 unknowns without any remeshing. The computational domain was the whole square domain. The initial design was the one in Fig. 2. There were 5 design variables and the optimized design is shown in Fig. 4. Both of the constraints (13) and (14) were involved where $\mathrm{B}^{\mathrm{avg}}_{\mathrm{min}} = 0.18\,\mathrm{T}$. The additional constraint (18) wasn't considered. The derivatives were computed by an analytical method of sensitivity analysis. This problem was solved by MATLAB's Optimization Toolbox [12] and we reached the result in 5 iterations.

The optimized design was produced and the measurements show significant improvements of the homogeneity. In Fig. 4 the magnetic induction along the

optimized designs α_{opt}	# of des. variables	# of unknowns	# of remeshs.	$\varphi_l(\alpha_0) \downarrow \varphi_l(\alpha_{\text{opt}})$	# of iters.	total CPU time [s]
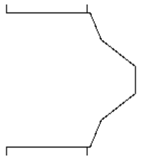	3	482	0	0.1068 $\downarrow$ 0.0144	29	37.96
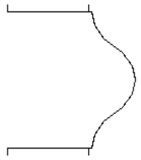	6	1237	3	0.1124 $\downarrow$ 0.0148	11–23	351.33
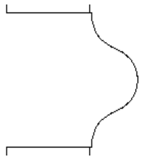	11	3207	21	0.1133 $\downarrow$ 0.0138	3–30	7905.82

Figure 5: Classical optimization strategy

polarization line is drawn. The homogeneity of the optimized computed field has improved by the factor 10, and even much more in the case of the measured field. Considering the state problem, we have observed that a nonlinear model should approximate the measurements very well.

4.3 Classical Optimization Strategy

We present 2D optimized designs of a different finesse computed by the classical optimization approach. The initial design α_0 can be seen in Fig. 6. The minimal magnetic induction was $\mathrm{B}_{\min}^{\text{avg}} = 0.25\,\mathrm{T}$ and the minimal curvature radius $\rho_{\min} = 1\,\mathrm{cm}$. Three approximations of the optimal design were calculated while started from the same initial design α_0. The results are resumed in Fig. 5. A weak point of the classical approach is that it requires many mesh regenerations for finer approximations.

The problem was computed by the software of SFB F013. Namely, we used a mesh generator NETGEN [9] for generation of an initial grid and all remeshings, a finite element package FEPP [3] for preprocessing of the state problem, algebraic multigrid package PEBBLES [8] for solving the state problem, and optimization tools built in FEPP which are based on the SQP method. Note that the state problem is solved by a direct method when it is not large.

level l	optimized designs α_l	# of des. variables	# of unknowns	# of remeshs.	$\varphi_l(\alpha_{l-1})$ $\downarrow$ $\varphi_l(\alpha_l)$	# of iters.	accumul. CPU time [s]
0 (init.)	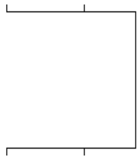	3	482		0.1068		
1	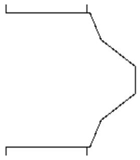	3	482	0	0.1068 $\downarrow$ 0.0144	29	37.96
2	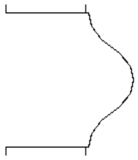	6	1457	0	0.0142 $\downarrow$ 0.0141	8	92.73
3	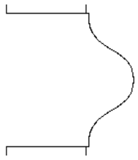	11	3403	0	0.0140 $\downarrow$ 0.0137	19	562.87

Figure 6: Hierarchical optimization strategy

4.4 Hierarchical Optimization Strategy

We also computed the 2D fine optimized design by the hierarchical optimization strategy. This strategy merely uses a coarse optimized design as an initial guess at the next finer level. The constraint parameters remain as in Sec. 4.3. The computation proceeded at 3 levels with 3, 6, and 11 design variables, respectively. Properties of the computation are presented in Fig. 6. As well as in Sec. 4.3, the problem was computed by the software tools of SFB F013. Additionaly we used the mesh generator NETGEN for generating a refined grid at each level of the hierarchical optimization.

Comparing to the classical approach, the hierarchical strategy is considerably faster, see the CPU times in Fig. 5 and Fig. 6. The main reason is that optimized designs on coarse grids approximate the ones on finer grids well. Consequently, there is no additional remeshing. In Fig. 6 we can also observe some convergence of the cost function $\varphi_l(\alpha_l)$ even if the discretized optimization problems at different levels are different. This convergence seems to be a natural criterion for a convergence of the whole algorithm.

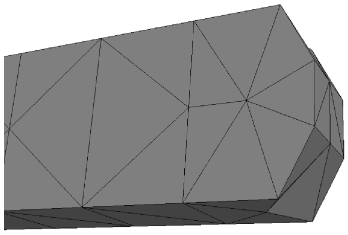

Figure 7: Optimized 3D shape

4.5 Optimized 3D Shape

At the end we present a first result computed in 3D. The state problem leads to a weak formulation in $H(\mathbf{rot})$ [3] which is being disretized by edge elements [4]. The number of unknowns was 2516. Considering the optimization, there were 4 design variables and the constraint parameter was $\mathrm{B}_{\mathrm{min}}^{\mathrm{avg}} = 0.2\,\mathrm{T}$. Since the constraint on minimal curvature for a coarse approximation has hardly any effect, it wasn't applied. We used the classical approach where 2 mesh regenerations were performed on account of flipped elements. The problem was computed by the SFB F013 software tools mentioned above. The optimized design can be seen in Fig. 7.

From a first glance it seems that the 2D optimized design is a good approximation of the 3D one. Thus, another step within the hierarchical optimization, namely approximation of a 3D initial design by a 2D optimized one, is straightforward.

5 Conclusions

We formulated a setting of the Maltese Cross problem in 2D. The 2D coarse optimized pole head was produced and the measurements have shown significant improvements of the homogeneity. We have found the hierarchical optimization strategy efficient for our problems. At last, the optimized coarse 3D result is quite similar to the 2D one which can be exploited in the hierarchical approach.

We have experienced with solving the problem in two different software environments. On the one hand, MATLAB [12] provides a comfortable debugging. On the other hand, the software of SFB F013 [3], [9], [8] is well designed to fit the problems governed a state equation and it also supports a hierarchical approach by mean of multigrid techniques. Moreover, the computations within the SFB F013 software were considerably faster comparing to MATLAB.

Following numbers of iterations in Secs. 4.2 and 4.3, we can see that the analytical methods of sensitivity analysis decreases the computational effort in a comparison to the numerical differentiation. By using of the analytical methods together with the hierarchical optimization approach, it seems that 3D problems of optimal shaping can be also solved efficiently.

References

[1] R. B. Brandtstätter, W. Ring, Ch. Magele, and K. R. Richter. Shape design with great geometrical deformations using continuously moving finite element nodes. *IEEE Transactions on Magnetics*, 34(5):2877–2880, September 1998.

[2] J. Haslinger and P. Neittaanmäki. *Finite Element Approximation for Optimal Shape Design: Theory and Applications.* John Wiley & Sons Ltd., Chinchester, 1988.

[3] M. Kuhn, U. Langer, and J. Schöberl. Scientific computing tools for 3d magnetic field problems. *The Mathematics of Finite Elements and Applications (MAFELAP X)*, pages 239–259, 2000.

[4] J. Nèdèlec. A new family of mixed finite elements in $\mathbf{R}^3$. *Numer. Math.*, 81:50–57, 1986.

[5] G. H. Peichl and W. Ring. Optimization of the shape of an electromagnet: Regularity results. *Advances in Mathematical Sciences and Applications*, 8:997–1014, 1998.

[6] G. H. Peichl and W. Ring. Asymptotic commutativity of differentiation and discretization in shape optimization. *Mathematical and Computing Modelling*, 29:19–37, 1999.

[7] J. Pištora, K. Postava, and R. Šebesta. Optical guided modes in sandwiches with ultrathin metallic films. *Journal of Magnetism and Magnetic Materials*, 198–199:683–685, 1999.

[8] S. Reitzinger. PEBBLES – user's guide. SFB "Numerical and Symbolic Scientific Computing", http://www.sfb013.uni-linz.ac.at.

[9] J. Schöberl. NETGEN - An advancing front 2D/3D-mesh generator based on abstract rules. *Comput.Visual.Sci*, pages 41–52, 1997.

[10] J. Sokolowski and J.-P. Zolesio. *Introduction to Shape Optimization.* Number 16 in Springer Series in Computational Mathematics. Springer, Berlin, 1992.

[11] N. Takahashi. Optimization of die press model. In *Proceedings of the TEAM Workshop in the Sixth Round*, Okayama, Japan, March 1996.

[12] The MathWorks, Inc. *MATLAB Optimization Toolbox User Manual*, 1993.